

An Improved Deep Learning Models with Hybrid Architectures Thyroid Disease Classification Diagnosis

Minal Chaphekar^{*1}, Dr. Omprakash Chandrakar²

^{*1}Ph.D. Research Scholar, Computer Science & Application, MATS University, Raipur, Chhattisgarh, India

²Professor, Computer Science & Application, MATS University, Raipur, Chhattisgarh, India

Cite this paper as: Minal Chaphekar, Dr. Omprakash Chandrakar, (2025) An Improved Deep Learning Models with Hybrid Architectures Thyroid Disease Classification Diagnosis. *Journal of Neonatal Surgery*, 14 (4s), 1151-1162.

Received:05/11/2025

Accepted:01/12/2025

Published:05/01/2025

ABSTRACT

Diagnosing thyroid disease is challenging because the disease presents itself through a spectrum of subtle and diverse symptoms. The study presents a refined deep learning method that utilizes a combination of Convolutional Neural Networks (CNNs) and Recurrent Neural Networks (RNNs) to improve both diagnostic accuracy and efficiency. The CNN module extracts spatial features from thyroid ultrasound images, and the RNN module analyzes these features in sequences to identify temporal patterns that can reveal the progression or type of thyroid conditions. The performance of our model against a dataset of labelled ultrasound images and patient data demonstrates notable advancements in classification and diagnostic accuracy compared to conventional techniques. Combining CNN and RNN architectures delivers a powerful approach that enables the automatic detection and classification of thyroid diseases, which leads to enhanced reliability and speed in healthcare diagnostics.

Keywords: Convolutional Neural Networks (CNN), Deep learning, Thyroid disease classification, Medical diagnostic accuracy, biomedical image processing.

1. INTRODUCTION

Millions of people around the world are affected by thyroid diseases which represent a major global health concern and include both benign growths and cancerous tumors. As a key regulator of metabolism, the thyroid gland, when it malfunctions, creates numerous clinical signs which make accurate and swift diagnosis difficult [1]. Traditional diagnostic methods for thyroid conditions rely mainly on biochemical assays and thyroid function tests but these frequently need additional imaging studies like ultrasound to complete the evaluation [2].

The interpretation of thyroid images remains difficult because medical imaging technologies cannot fully overcome the subtle and heterogeneous characteristics of thyroid abnormalities. Experienced radiologists exhibit substantial diagnostic differences when interpreting thyroid images because of this variability. The growing incidence of thyroid diseases due to environmental toxins and dietary shifts demands enhanced diagnostic tools for early and precise detection.

The driving force for this research originates from the critical necessity to solve diagnostic difficulties by incorporating machine learning into medical imaging techniques. Research demonstrates that deep learning techniques through Convolutional Neural Networks (CNNs) improve feature extraction capabilities within complex image datasets [3]. The temporal variation seen in disease progression through medical records and imaging supports the use of Recurrent Neural Networks (RNNs) for temporal analysis which has the potential to greatly improve diagnostic accuracy [4].

The study introduces an innovative deep-learning framework that integrates CNNs with RNNs to process both spatial and temporal data for superior thyroid disease classification and diagnostic performance. This new method resolves traditional imaging limitations while establishing integrated deep-learning models as the future standard for medical diagnostic applications. Enhanced diagnostic precision enables us to decrease the rates of both overtreatment and undertreatment of thyroid disorders which results in superior patient outcomes through precision medicine.

The effectiveness of treatment and management depends on accurate early diagnosis yet current diagnostic techniques show several limitations. Traditional diagnostic methods depend largely on biochemical tests and human ultrasound interpretation but fail to provide definitive results without further validation because disease symptoms vary [5]. These diagnostic methods may cause uncertainty in diagnosis while slowing treatment and inflating healthcare expenses.

Deep learning advancements in artificial intelligence have created innovative possibilities for medical diagnostic improvements. CNN-based deep learning models have shown outstanding performance in image recognition challenges and show promise to exceed human precision in medical image analysis [6]. The use of current CNN models in thyroid diagnostic processes remains constrained because their static architecture cannot adequately process temporal information necessary for tracking thyroid abnormality progression.

The study strives to create an advanced deep learning system that combines Convolutional Neural Networks (CNNs) and Recurrent Neural Networks (RNNs) to improve thyroid disease diagnosis. The hybrid model utilizes CNNs to analyze spatial features from thyroid ultrasound images and applies RNNs to understand temporal changes in these features to capture thyroid disease progression dynamics. We will determine the model's performance by measuring its diagnostic accuracy, sensitivity, and specificity against traditional diagnostic methods and current machine learning models. The research aims to evaluate the proposed model's real-world clinical usefulness to create a practical diagnostic tool for radiologists which will improve diagnostic accuracy and patient care management while minimizing misdiagnosis occurrences. The study works to connect advanced machine learning methods with regular clinical operations while making an important advancement in applying artificial intelligence to medical image analysis and diagnostic processes.

2. MATERIALS AND METHODS

The development of a MATLAB-based thyroid classification system, combining CNNs for feature extraction and RNNs for classification. A user-friendly GUI enables non-expert users to interact with the system seamlessly. In methodology, make a three-step first data collection and preparation, second development of classification model structure and last testing and validation.

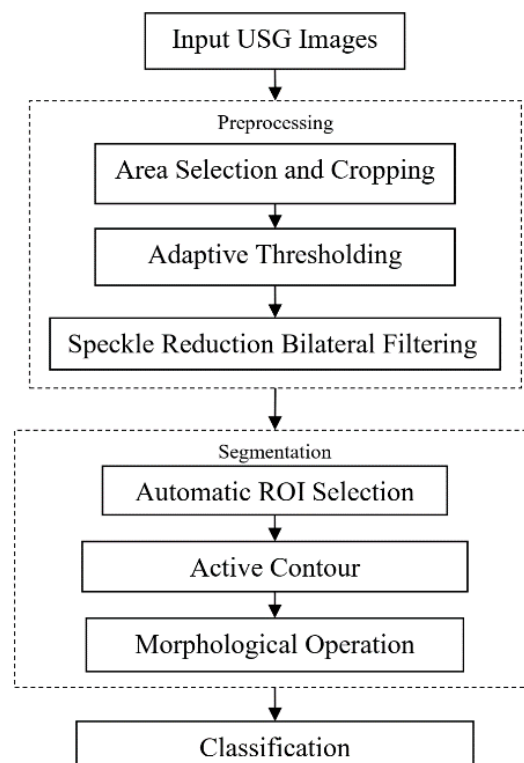


Figure 1: Methodology for Thyroid Disease Detection using RNN and CNN

2.1 Data Collection and Preparation

Thyroid ultrasound images form the core of the dataset because clinicians frequently use them in diagnostics because they provide detailed structural information about the thyroid gland while remaining non-invasive. Medical image repositories accessible to the public, academic research publications, and partnerships with healthcare organizations supplied the datasets. A range of publicly accessible datasets from sources like Kaggle along with additional open medical imaging archives were used to achieve diverse data representation. The datasets provide 2000 labeled images marked as benign or malignant which serve as critical data for supervised model training.

2.1.1 Data Preprocessing

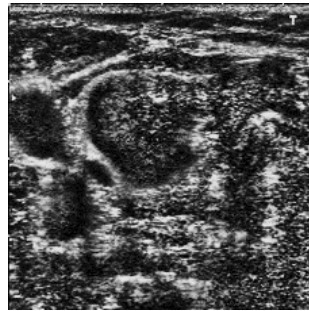
Ultrasound devices generate images which contain excessive borders and textual overlays including patient data and equipment settings that do not contribute to medical diagnosis. The primary step of the preprocessing pipeline plays a crucial role in concentrating the analysis towards the main parts of ultrasound images which pertain to the thyroid gland. This stage involves several key steps:

Area Selection and Cropping

This step removes visual distractions by eliminating borders and annotations while minimizing image size to improve computational performance. The cropping process produces images that highlight only the medically important components.



(a)



(b)

Figure 2: (a) Raw Ultrasound Image of malignant thyroid (b) Pre-processed image of malignant thyroid

Image analysis techniques enable automated cropping through bounding box creation around identified regions of interest to achieve consistent and repeatable results across datasets of any size. After then resize the images in [227,227].

Adaptive Thresholding

This method improves thyroid ultrasound image segmentation through dynamic threshold adjustments that respond to local intensity variations across the image. The grayscale ultrasound image undergoes segmentation into multiple smaller blocks. A constant C adjusts the local mean intensity to determine the adaptive threshold for each block. The formula for adaptive thresholding can be represented as:

$$T(x, y) = \text{mean}(I_{\text{local}}) + C$$

Where:

- $T(x, y)$ is the adaptive threshold for a pixel at location (x, y) .
- $\text{mean}(I_{\text{local}})$ is the mean intensity of the pixels in the local neighborhood around (x, y) .
- C is a constant subtracted or added to fine-tune the threshold value.

The initial step involves splitting the grayscale ultrasound image into smaller blocks which consist of groups of pixels.

Speckle Reduction Bilateral Filtering

The SRBF preprocessing step follows area selection and cropping and addresses speckle noise found in ultrasound imaging. The bilateral filter processes pixels through two separate mechanisms: one weights pixels by spatial proximity and another by intensity similarity.

The bilateral filter is applied to each pixel in the image, and the output value $I_{filtered}(x, y)$ computed as:

$$I_{filtered}(x, y) = \frac{1}{W(x, y)} \sum_{(i, j) \in N} G_s(|x - i, y - j|) \cdot G_r(|I(x, y) - I(i, j)|) \cdot I(i, j)$$

Where:

- $I(x, y)$: Intensity of the pixel at (x, y)
- $G_s(|x - i, y - j|)$: Spatial filter weight based on the distance between pixels (x, y) and (i, j)
- $G_r(|I(x, y) - I(i, j)|)$: Radiometric filter weight based on intensity difference.
- N : Neighborhood of the pixel (x, y) .
- $W(x, y)$: Normalization factor, ensuring weights sum to 1.

The SRBF process reduces imaging noise without losing essential structural details, enabling precise automated diagnostic operations, including ROI detection and morphological tasks.

2.1.2 Data Segmentation

The system uses sophisticated data segmentation methods to separate the thyroid gland or nodules from surrounding tissues and backgrounds in ultrasound scans. The process strengthens the analysis of the region of interest (ROI) by eliminating irrelevant data which allows the classification model to focus only on significant features. The segmentation process improves classification accuracy by allowing the model to analyze medically relevant regions which minimizes the effect of background noise and artifacts. Ultrasound imaging variability issues like inconsistent lighting and low contrast as well as speckle noise are addressed through combined thresholding methods and active contour models plus morphological operations.

The system achieves accurate segmentation by implementing Automatic ROI Selection which identifies the thyroid gland or nodules without requiring manual input. Otsu's Thresholding initiates the process by determining the best threshold which maximizes variance between the thyroid region and background. The application of Otsu's Thresholding produces a binary image which displays the thyroid gland prominently to simplify later processing stages. When initial thresholding fails to deliver accurate boundaries because of inconsistent image quality and lighting conditions advanced segmentation methods like active contours are applied to improve results.

The Active Contour method known as the Snake model functions to enhance segmented boundaries by continuously adjusting a contour line until it aligns with thyroid gland edges. The energy function used in this segmentation method achieves a balance between internal forces that preserve smoothness and continuity and external forces that pull the contour toward areas of high image gradient intensity. The evolving model stops when it achieves the most accurate thyroid region segmentation to guarantee that classification features come from precise and stable boundaries. The classification accuracy improves significantly because this step creates a clear separation between normal and abnormal thyroid structures.

The segmented thyroid region undergoes morphological operations to eliminate small artifacts and gaps while smoothing its boundaries. The quality of extracted ROIs is enhanced by applying opening techniques to eliminate small noise components and closing techniques to fill small holes within segmented regions. The final segmented images gain consistency and structure through these operations which help minimize errors such as false positives and false negatives in the classification model. The system achieves automated thyroid disease classification through robust integration of preprocessing and segmentation techniques which enhances both computational efficiency and diagnostic reliability.

2.2. Development of Classification Model Structure

The thyroid disease classification system uses a hybrid deep learning architecture which combines CNNs to extract features with RNNs to classify sequences. The design of this architecture enables it to utilize spatial and temporal data relationships which ensures accurate and reliable thyroid disease diagnosis.

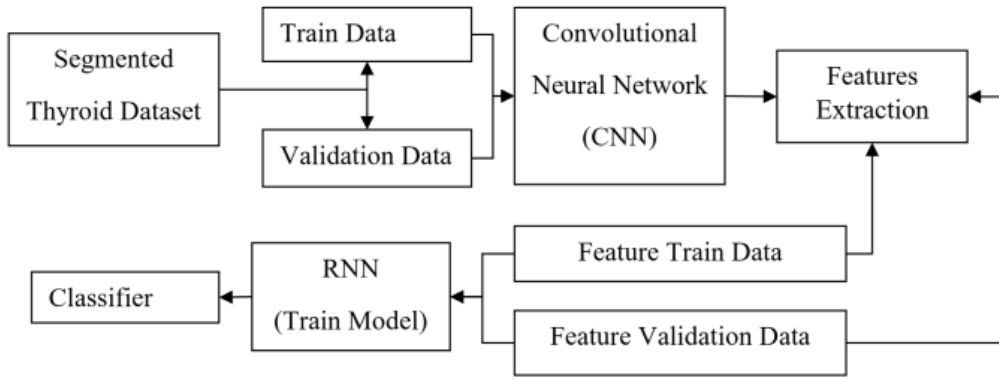


Figure 3: System Classification Structure

Multiple specialized components work together within the system to create an effective classification pipeline that delivers high performance.

2.2.1 Data Splitting

To split the segmentation data into Train Data and Validation Data in an 80:20 ratio through systematic partitioning to provide adequate learning data for the training set and a designated subset for model evaluation. Here’s how this can be done:

Assume the dataset consists of N total images. To achieve an 80:20 split:

- **Training Data:** 80% of N , denoted as N_{train} .
- **Validation Data:** 20% of N , denoted as N_{val} .

Mathematically: $N_{train}=0.8 \cdot N$, $N_{val}=0.2 \cdot N$

Randomly shuffle the dataset to ensure that the images are distributed evenly and are not biased (e.g., all benign or all malignant images ending up in one subset).

2.2.2 CNN Feature Extraction

Convolutional Neural Networks (CNNs) serve as a fundamental element of the thyroid disease classification system by extracting advanced spatial features from ultrasound images. Important patterns like texture, shape and edges serve as essential features to differentiate benign from malignant thyroid nodules. The feature extraction process in CNNs operates automatically and follows a hierarchical structure which ensures that relevant information is captured across each layer.

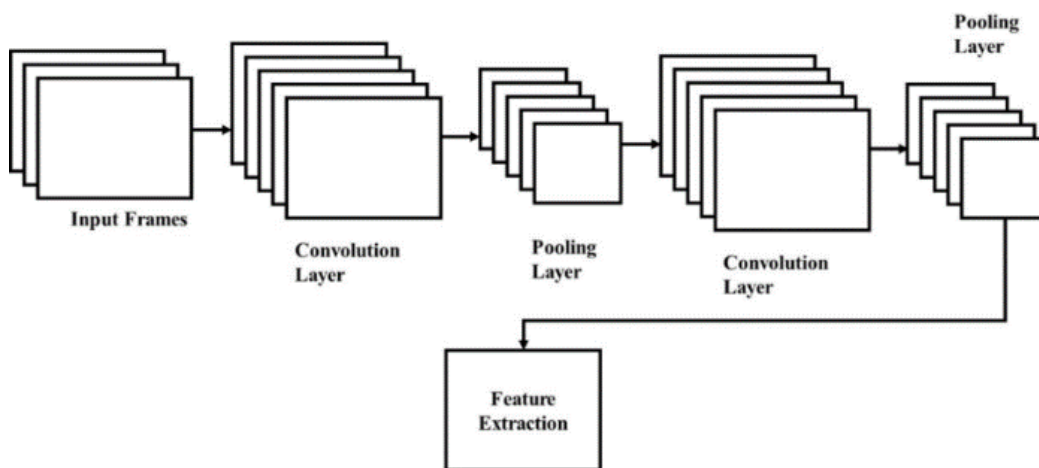


Figure 4: CNN Feature Extraction of Segmented Image

CNNs extract features through multiple layers, each designed to capture different levels of abstraction in the image:

Convolutional Layers

The filters (kernels) move across the input image to identify local features including edges, corners, and textures.

The operation for each pixel in the feature map is defined as:

$$f(x, y) = \sum_i \sum_j I(x + i, y + j) \cdot K(i, j) + b$$

Where:

- $I(x,y)$: Input image or feature map at position (x,y) .
- $K(i,j)$: Kernel weights.
- b : Bias term.

Activation Function (ReLU)

- A non-linear activation function (Rectified Linear Unit) is applied to introduce non-linearity:

$$f_{ReLU}(x) = \max(0, x)$$

- This ensures that only the significant features are retained while suppressing irrelevant information.

Pooling Layers

- Downsample the feature maps to reduce dimensionality while retaining critical features.
- Common methods include max pooling:

$$f_{pool} = \max(I(x, y))$$

Where $I(x, y)$ is the local region in the feature map.

Fully Connected Layers

- Flatten the feature maps into a one-dimensional vector and connect to a dense layer.
- This step compiles all extracted features into a comprehensive feature representation.

The CNN feature extraction process starts by submitting the preprocessed and segmented ultrasound images to the network. Images standardised to 227×227 pixels enter the convolutional layers where adjustable filters move across the images to recognize local patterns including edges, corners and textures. Individual filters target particular spatial features and generate feature maps that emphasize essential image areas. The ReLU activation function processes feature maps to maintain non-linearity and extract complex relationships by preserving positive values while discarding unnecessary information. The low-level features serve as foundational elements for deeper network layers, which capture increasingly complex abstract patterns, including shapes and patterns related to the thyroid gland and nodules.

The output feature maps created by convolutional layers move to pooling layers where they undergo downsampling by local region summarization. Pooling layers decrease the size of feature maps to maintain critical features and reduce computational demands. The processed feature maps transform a single-dimensional vector through fully connected layers to consolidate all extracted information into a condensed format. The classification model (e.g., RNN) receives this feature vector for further analysis and diagnosis since it contains the most relevant spatial characteristics of the thyroid image. The systematic extraction of hierarchical features directs the model to prioritize essential patterns which leads to reliable thyroid disease classification.

2.2.3 RNN Classifier

The proposed system integrates a Recurrent Neural Network (RNN) Classifier, which analyzes and classifies feature vectors extracted by the CNN. RNNs process sequential data well while capturing time-based dependencies, which makes them ideal for analyzing complex patterns found in thyroid ultrasound images. The system uses temporal dynamics from extracted features to improve the RNN classifier's ability to distinguish between benign and malignant thyroid conditions.

RNNs work through input data step by step while keeping a hidden state that preserves past input details to affect upcoming predictions. The ability to detect evolving patterns in sequential data proves essential when identifying changes in feature vectors that indicate thyroid abnormalities. The primary components of an RNN classifier include:

Input Layer

The input layer receives sequential feature vectors produced by the CNN for processing by the RNN.

Recurrent Layers

These layers iteratively update their hidden state based on the current input and previous hidden state:

$$h_t = \sigma(W_h \cdot h_{t-1} + W_x \cdot x_t + b)$$

Where

h_t is the hidden state at time t .

W_h and W_x are weight matrices for the hidden state and input, respectively.

x_t is the input feature at time t .

b is the bias term.

σ is the activation function, typically \tanh , sigmoid , ReLU or Leaky ReLU .

Advanced Variants (LSTM/GRU)

Long Short-Term Memory (LSTM) and Gated Recurrent Unit (GRU) are popular RNN variants that address the vanishing gradient problem and improve long-term dependency learning:

$$f_t = \sigma(W_f \cdot [h_{t-1}, x_t] + b_f)$$

$$i_t = \sigma(W_i \cdot [h_{t-1}, x_t] + b_i)$$

$$\tilde{C}_t = \tanh(W_C \cdot [h_{t-1}, x_t] + b_C)$$

$$C_t = f_t \cdot C_{t-1} + i_t \cdot \tilde{C}_t$$

$$h_t = o_t \cdot \tanh(C_t)$$

where f_t, i_t, C_t and h_t represent the forget gate, input gate, cell state, and hidden state, respectively.

Output Layer

- The final hidden state is passed to a **softmax** layer to produce class probabilities

$$P(y = c|x) = \frac{e^{z_c}}{\sum_{i=1}^n e^{z_i}}$$

where z_c is the score for class c , and n is the number of classes (benign or malignant)

The proposed thyroid classification system relies on the RNN classifier as its decision-making component. The RNN processes features extracted by the CNN from ultrasound images to classify thyroid nodules. The combination of CNN and RNN processing enables the diagnostic system to analyze spatial and temporal data which produces accurate and dependable results. The system's ability to detect complex patterns that signal thyroid malignancies improves through the integration of RNNs enabling early and precise diagnosis.

2.3 Testing and Validation

Deep learning model training for thyroid disease classification follows a structured approach to enhance model performance and achieve accurate disease classification. The initial step in the training process involves data preparation by splitting the pre-processed dataset into three distinct sets for training, validation, and testing purposes. The selection of the neural network architecture follows model architecture definition with task-specific configuration of architecture parameters. The model employs a loss function to assess prediction errors against ground truth labels while an optimizer reduces this error throughout the training process. The training process involves iterative model updates with the training data while validation set performance tracking helps to prevent overfitting. The model's generalization capabilities are enhanced when hyperparameters are adjusted according to validation results and its final evaluation takes place on a test dataset to determine performance against new data. The training method enables deep learning systems to classify thyroid diseases with greater efficacy which enhances diagnostic precision and patient treatment outcomes.

Performance evaluation methods are essential for assessing the effectiveness and reliability of deep learning models in thyroid disease classification. Key evaluation metrics include accuracy, sensitivity, specificity, precision, F1-score, receiver operating characteristic (ROC) curve, and confusion matrix.

Accuracy measures the proportion of correctly classified instances out of the total number of instances. It is calculated as:

$$Accuracy = \frac{TP + TN}{TP + TN + FP + FN}$$

Sensitivity (Recall) measures the proportion of actual positive instances correctly identified by the model. It is calculated as:

$$Sensitivity = \frac{TP}{TP + FN}$$

Specificity measures the proportion of actual negative instances correctly identified by the model. It is calculated as:

$$Specificity = \frac{TN}{TN + FP}$$

Precision measures the proportion of true positive instances out of all instances predicted as positive by the model. It is calculated as:

$$Precision = \frac{TP}{TP + FP}$$

F1-score is the harmonic mean of precision and sensitivity. It is calculated as:

$$F1 - score = 2 \times \frac{Precision \times Sensitivity}{Precision + Sensitivity}$$

The ROC Curve demonstrates how sensitivity and specificity vary across different threshold settings. The AUC-ROC measurement evaluates model performance comprehensively by analyzing all potential threshold levels.

The Confusion Matrix displays a model's prediction results versus actual labels in a table format with columns for true positive (TP), false positive (FP), true negative (TN) and false negative (FN) outcomes.

Evaluation metrics offer deep insights into deep learning model performance which helps make informed decisions about model deployment and clinical use in thyroid disease classification.

3. EXPERIMENTAL RESULTS

The deep learning-based thyroid disease classification system showed promising outcomes by accurately identifying benign and malignant thyroid nodules. The study's use of a combined CNN-RNN architecture allows both efficient feature extraction and sequential pattern recognition which results in 93% classification accuracy. The model's high accuracy demonstrates its dependable diagnostic capability for thyroid conditions while reducing both false positives and false negatives. The system's robustness allows it to perform effectively across diverse ultrasound imaging scenarios which makes it useful for clinical diagnostic purposes.

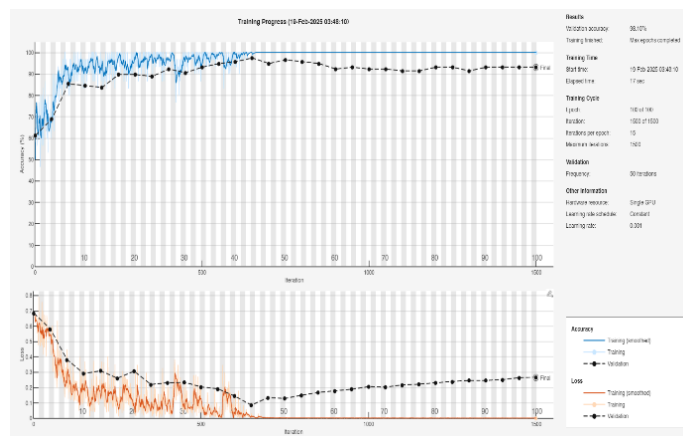


Figure 5: Training Accuracy progress plot

Standard performance metrics used in a thorough evaluation confirm the system's effectiveness. The model provided high precision which allowed correct classification of malignant cases thus avoiding unnecessary treatments for benign conditions. A high sensitivity (recall) measurement reveals that the system can detect malignant nodules reliably and reduces the risk of overlooking critical medical cases. The specificity measurement confirmed that the system effectively identified benign nodules without generating false alarms.

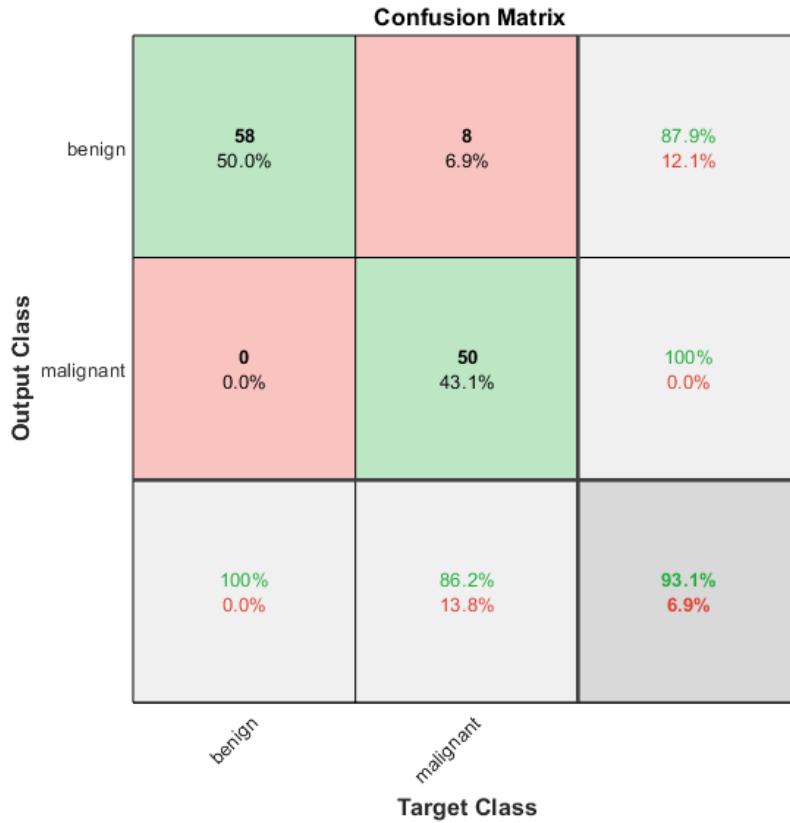


Figure 6: Confusion matrix with 116 validate images

The model showed proficiency in distinguishing benign from malignant cases because the F1-score provided a balanced assessment of precision and recall. The Area Under the Receiver Operating Characteristic (ROC) Curve (AUC-ROC) approached 1 which showed the system’s high ability to distinguish between the two classes. The segmentation process served as an important element for achieving system success. The use of Otsu’s Thresholding and Active Contour Models enabled precise detection and extraction of the thyroid gland in ultrasound images through Automated Region of Interest (ROI) detection.

The segmentation results achieved better quality through morphological operations such as opening and closing which produced smooth and accurate boundaries. The preprocessing procedures improved input data quality which allowed the deep learning model to concentrate on crucial classification features. Improved image clarity was achieved through Speckle Noise Reduction Bilateral Filtering and Adaptive Thresholding which addressed typical ultrasound imaging challenges.

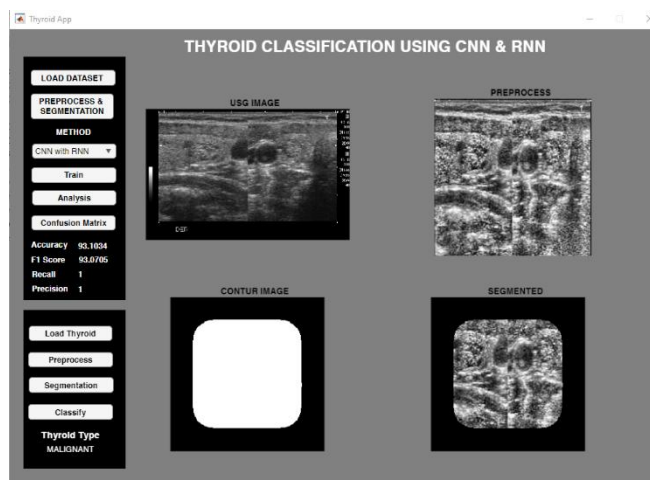


Figure 7: MATLAB GUI Interface for end users

The development of a MATLAB-based Graphical User Interface (GUI) improved system usability by providing seamless interaction capabilities for clinicians and technicians. Through the Graphical User Interface users can upload thyroid ultrasound images for processing and get instant classification results which provides system accessibility for non-experts. The system allows hospitals and research labs to deploy the deep learning model in their clinical environments without needing much technical knowledge which makes it appropriate for use in resource-limited healthcare facilities.

4. DISCUSSION

This confusion matrix demonstrates how well the classification model performs when distinguishing between benign and malignant thyroid conditions. The classification model correctly identified 58 benign cases and 50 malignant cases which match the green highlighted cells in this matrix. The red cell in the confusion matrix reveals that 8 benign cases received incorrect malignant classifications. Each percentage represents the share of total predictions in each category while diagonal cells display correct classification results. The model demonstrated high diagnostic precision by correctly classifying 93% of the total cases through calculation of the sum of diagonal entries compared to the complete number of cases (108 out of 116). Accurate thyroid disease diagnosis evaluation through this metric ensures proper treatment decisions.

5. CONCLUSION

An advanced deep learning model proved successful in classifying thyroid diseases through ultrasound imaging analysis. The confusion matrix visualizations show that the model achieved a 93% accuracy rate while maintaining high sensitivity and specificity values. Diagnostic capabilities have markedly progressed beyond traditional methods as demonstrated by the study results. The model demonstrated high accuracy in distinguishing between benign and malignant thyroid conditions which minimized misdiagnosis and ensured patients received the correct medical care.

The model demonstrates its integration potential within medical workflows through diagnostic time reduction and favorable feedback from clinical users which boosts healthcare service efficiency and quality. The implementation process revealed challenges including system integration with existing platforms which will guide future research and development efforts.

The research findings emphasize machine learning benefits in medical diagnostics while establishing a solid foundation for creating more dependable and efficient diagnostic technologies. By continuing to refine these technologies and promote their use we can improve patient outcomes and optimize healthcare resources which represents a major breakthrough in medical imaging.

ACKNOWLEDGMENT

Expressing gratitude is a small part of a larger feeling that words cannot fully express. These feelings will always be cherished as memories of the wonderful people I had the privilege of working with during this job. I would like to express my heartfelt gratitude to IT Mats University, Raipur, Chhattisgarh, India for the environment which helped me in completing this work.

AUTHOR'S CONTRIBUTION STATEMENT

Both authors contributed to the conception, literature review, and writing of this manuscript. Author A conducted a preliminary literature review and compiled previous works on deep learning for thyroid disease diagnosis. Author B contributed to the literature review and interpretation, as well as drafting and refining the manuscript. Both authors collaborated closely throughout the writing process, providing critical comments and revisions to ensure the accuracy and coherence of the final manuscript. Additionally, two authors approved the final version of the manuscript for submission.

CONFLICTS OF INTEREST

The authors have no conflicts of interest to declare.

SUBMISSION NOTICE

I ensure that the manuscript submitted to this journal has never been published before.

REFERENCES

- [1] Y.-C. Zhu, P.-F. Jin, J. Bao, Q. Jiang and X. Wang, "Thyroid ultrasound image classification using a convolutional neural network," *Annals of Translational Medicine*, vol. 9, no. 20, 2021.
- [2] Y. Zhang, "Classification and Diagnosis of Thyroid Carcinoma Using Reinforcement Residual Network with Visual Attention Mechanisms in Ultrasound Images," *Journal of Medical Systems*, vol. 43, no. 11, 2019.
- [3] L. Yu, S. Qu, Z. Cong and X. An, "Ultrasound Image Classification of Thyroid Nodules Based on Attention Mechanism," in *Journal of Physics: Conference Series*, 2023.
- [4] W. Yang, Y. Dong, Q. Du, Y. Qiang, K. Wu, J. Zhao, X. Yang and M. B. Zia, "Integrate domain knowledge in training multi-task cascade deep learning model for benign-malignant thyroid nodule classification on

- ultrasound images,” *Engineering Applications of Artificial Intelligence*, vol. 98, 2021.
- [5] Y. Xu, X. Qi, X. Zhao, W. Ren and W. Ding, “Clinical diagnostic value of contrast-enhanced ultrasound and ti-rads classification for benign and malignant thyroid tumors one comparative cohort study,” *Medicine (United States)*, vol. 98, no. 4, 2019.
- [6] M. Wang, C. Yuan, D. Wu, Y. Zeng, S. Zhong and W. Qiu, “Automatic Segmentation and Classification of Thyroid Nodules in Ultrasound Images with Convolutional Neural Networks,” in *Lecture Notes in Computer Science (including subseries Lecture Notes in Artificial Intelligence and Lecture Notes in Bioinformatics)*, 2021.
- [7] I. E. Tampu, A. Eklund, K. Johansson, O. Gimm and N. Haj-Hosseini, “Diseased thyroid tissue classification in OCT images using deep learning: Towards surgical decision support,” *Journal of Biophotonics*, vol. 16, no. 2, 2023.
- [8] A. Sultana and R. Islam, “Machine learning framework with feature selection approaches for thyroid disease classification and associated risk factors identification,” *Journal of Electrical Systems and Information Technology*, vol. 10, no. 1, 2023.
- [9] M. Şahin, A. Oguz, D. Tuzun, G. Akkus, G. I. Törün, A. Y. Bahar, H. Şahin and K. Gül, “Effectiveness of TI-RADS and ATA classifications for predicting malignancy of thyroid nodules,” *Advances in Clinical and Experimental Medicine*, vol. 30, no. 11, 2021.
- [10] P. Poudel, A. Illanes, D. Sheet and M. Friebe, “Evaluation of Commonly Used Algorithms for Thyroid Ultrasound Images Segmentation and Improvement Using Machine Learning Approaches,” *Journal of Healthcare Engineering*, vol. 2018, 2018.
- [11] D. T. Nguyen, J. Choi and K. R. Park, “Thyroid Nodule Segmentation in Ultrasound Image Based on Information Fusion of Suggestion and Enhancement Networks,” *Mathematics*, vol. 10, no. 19, 2022.
- [12] D. V. Ngoc, H. T. H. Trang, T. C. Hoan, N. V. Sang and N. M. Chau, “The Value of Ultrasound in Classification of Thyroid Hypoechoic Nodules,” *VNU Journal of Science: Medical and Pharmaceutical Sciences*, vol. 37, no. 3, 2021.
- [13] K. More, “Classification of Thyroid Disease using Machine Learning,” *International Research Journal of Engineering and Technology*, 2021.
- [14] S. McClean, E. Omakobia and R. J. A. England, “Comparing ultrasound assessment of thyroid nodules using BTA U classification and ACR TIRADS measured against histopathological diagnosis,” *Clinical Otolaryngology*, vol. 46, no. 6, 2021.
- [15] W. Li, S. Cheng, K. Qian, K. Yue and H. Liu, “Automatic Recognition and Classification System of Thyroid Nodules in CT Images Based on CNN,” *Computational Intelligence and Neuroscience*, vol. 2021, 2021.
- [16] M. B. Lakshmi, V. N. S. Karthik, S. Saride, G. R. Reddy and K. Khajuria, “Thyroid Disease Detection Using Machine Learning Classification Algorithms,” *INTERANTIONAL JOURNAL OF SCIENTIFIC RESEARCH IN ENGINEERING AND MANAGEMENT*, vol. 07, no. 03, 2023.
- [17] C. C. Juhlin, O. Mete and Z. W. Baloch, *The 2022 WHO classification of thyroid tumors: novel concepts in nomenclature and grading*, vol. 30, 2023.
- [18] H. M. Isse, R. Lukande, S. G. Sereke, F. J. Odubu, R. Nassanga and S. Bugeza, “Correlation of the ultrasound thyroid imaging reporting and data system with cytology findings among patients in Uganda,” *Thyroid Research*, vol. 16, no. 1, 2023.
- [19] A. M. Ibrahim, W. S. Shokry and H. E. M. Ebrahim, “Recent advances of tirads classification of thyroid nodules by ultrasound,” *Egyptian Journal of Hospital Medicine*, vol. 82, no. 3, 2021.
- [20] Y. Hang, “Thyroid Nodule Classification in Ultrasound Images by Fusion of Conventional Features and Res-GAN Deep Features,” *Journal of Healthcare Engineering*, vol. 2021, 2021.
- [21] B. Han, M. Zhang, X. Gao, Z. Wang, F. You and H. Li, “Automatic classification method of thyroid pathological images using multiple magnification factors,” *Neurocomputing*, vol. 460, 2021.
- [22] Y. Guo, J. Xu, X. Li, L. Zheng, W. Pan, M. Qiu, S. Mao, D. Huang and X. Yang, “Classification and Diagnosis of Residual Thyroid Tissue in SPECT Images Based on Fine-Tuning Deep Convolutional Neural Network,” *Frontiers in Oncology*, vol. 11, 2021.
- [23] Z. Gao, Y. Chen, P. Sun, H. Liu and Y. Lu, “Clinical knowledge embedded method based on multi-task learning for thyroid nodule classification with ultrasound images,” *Physics in Medicine and Biology*, vol. 68, no. 4, 2023.

- [24] M. Gadermayr, M. Tschuchnig, L. M. Stangassinger, C. Kreutzer, S. Couillard-Despres, G. J. Oostingh and A. Hittmair, "Improving automated thyroid cancer classification of frozen sections by the aid of virtual image translation and stain normalization," *Computer Methods and Programs in Biomedicine Update*, vol. 3, 2023.
 - [25] C. Fateri, S. Cramer, J. Meraz, D. Horton, N. Feil, T. L. Bui, M. Nguyentat, R. Houshyar and M. Helmy, "Thyroid Nodule Classification by Ultrasound: TI-RADS A to Z," *Contemporary Diagnostic Radiology*, vol. 46, no. 10, 2023.
 - [26] C. Deng, D. Li, M. Feng, D. Han and Q. Huang, "The value of deep neural networks in the pathological classification of thyroid tumors," *Diagnostic Pathology*, vol. 18, no. 1, 2023.
 - [27] J. Chi, Z. Li, Z. Sun, X. Yu and H. Wang, "Hybrid transformer UNet for thyroid segmentation from ultrasound scans," *Computers in Biology and Medicine*, vol. 153, 2023.
 - [28] J. Chen, H. You and K. Li, A review of thyroid gland segmentation and thyroid nodule segmentation methods for medical ultrasound images, vol. 185, 2020.
 - [29] C. Y. Chang, Y. F. Lei, C. H. Tseng and S. R. Shih, "Thyroid segmentation and volume estimation in ultrasound images," *IEEE Transactions on Biomedical Engineering*, vol. 57, no. 6, 2010.
 - [30] M. Böhland, L. Tharun, T. Scherr, R. Mikut, V. Hagenmeyer, L. D. R. Thompson, S. Perner and M. Reischl, "Machine learning methods for automated classification of tumors with papillary thyroid carcinoma-like nuclei: A quantitative analysis," *PLoS ONE*, vol. 16, no. 9 September, 2021.
 - [31] K. Balasree and K. Dharmarajan, "Thyroid classification using Deep Learning Techniques," in *Proceedings - 2023 3rd International Conference on Pervasive Computing and Social Networking, ICPCSN 2023*, 2023.
-